

# Gallic acid-iron complex modified magnesium hydroxide and its effect on flame retardancy of EVA



Tao Wang<sup>a,1</sup>, Dong-Wei Yao<sup>a,1</sup>, Guang-Zhong Yin<sup>b,c,\*</sup>, Yan Jiang<sup>a,d</sup>, Na Wang<sup>a,d</sup>, De-Yi Wang<sup>b,c,\*\*</sup>

<sup>a</sup> Liaoning Provincial Key Laboratory for Synthesis and Preparation of Special Functional Materials, Shenyang University of Chemical Technology, Shenyang, 110142, China

<sup>b</sup> Escuela Politécnica Superior, Universidad Francisco de Vitoria, Ctra. Pozuelo-Majadahonda Km 1,800, 28223, Pozuelo de Alarcón, Madrid, Spain

<sup>c</sup> IMDEA Materials Institute, C/ Eric Kandel, 2, 28906, Getafe, Madrid, Spain

<sup>d</sup> Shenyang Research Institute of Industrial Technology for Advanced Coating Materials, Shenyang, 110142, China

## ARTICLE INFO

### Article history:

Received 1 November 2022

Received in revised form

8 December 2022

Accepted 19 December 2022

### Keywords:

Ethylene-vinyl acetate copolymer (EVA)

Surface modification

Flame retardancy

Magnesium hydroxide (MH)

## ABSTRACT

In this paper, a green method of modifying high flame retardant and high mechanical properties MH was proposed, gallic acid (GA)-Fe<sup>3+</sup> complex was employed to modify the surface of magnesium hydroxide (MH), aiming to achieve novel functionalized MH-based flame retardant for ethylene-vinyl acetate copolymer (EVA). The structural and morphological characterization of the newly designed flame retardant were studied by Fourier transform infrared spectroscopy, X-ray photoelectron spectroscopy, Scanning electron microscope and X-ray Diffraction. The flame retardancy of EVA, EVA/MH, EVA/MH@Fe-GA was investigated via Limiting oxygen index, UL-94 vertical combustion tests, and cone calorimeter test. The LOI and UL94 results showed that EVA/MH@Fe-GA (01) achieved an LOI of 38.5% and UL-94 passed the V-0 grade. The CCT results showed that compared with neat EVA, the peak heat release rate (pHRR) of EVA/MH@Fe-GA decreased by 90.83%, and TSP decreased by 86%, as compared to neat EVA. The mechanical properties of EVA/MH, EVA/MH@Fe-GA were investigated via tensile and impact tests. Compared with EVA/MH, MH@GA-Fe shows good tensile property and impact resistance, the impact strength of EVA/MH@Fe-GA increased by more than 28%, and the elongation at break increased by 145%.

© 2022 Kingfa Scientific and Technological Co. Ltd. Publishing services by Elsevier B.V. on behalf of KeAi Communications Co. Ltd. This is an open access article under the CC BY license (<http://creativecommons.org/licenses/by/4.0/>).

## 1. Introduction

Ethylene-vinyl acetate copolymer (EVA), possessing different vinyl acetate (VA) contents, has been used in various fields such as electronic engineering, cable industry and foaming material [1–3]. However, two important disadvantages of EVA are particularly flammable and emit a significant local smoke during burning [4,5].

\* Corresponding author. Escuela Politécnica Superior, Universidad Francisco de Vitoria, Ctra. Pozuelo-Majadahonda Km 1,800, 28223, Pozuelo de Alarcón, Madrid, Spain

\*\* Corresponding author. Escuela Politécnica Superior, Universidad Francisco de Vitoria, Ctra. Pozuelo-Majadahonda Km 1,800, 28223, Pozuelo de Alarcón, Madrid, Spain

E-mail addresses: [amos.guangzhong@ufv.es](mailto:amos.guangzhong@ufv.es) (G.-Z. Yin), [deyi.wang@imdea.org](mailto:deyi.wang@imdea.org) (D.-Y. Wang).

<sup>1</sup> These authors contributed equally to this work.

In order to solve these two problems so that EVA can be used more widely, it is particularly important to improve the flame retardancy properties of EVA. A common method is to introduce flame retardants, such as magnesium hydroxide (MH) [6,7].

MH is an excellent non-toxic and smoke-suppressing flame retardant because of its decomposition temperature (about 340 °C, being higher than that of aluminum hydroxide), smoke suppressibility, non-toxicity, and wide use in halogen-free polymer materials [8–11]. However, due to strong polarity, easy polymerization, hydrophilicity and oil repellency, and low flame retardant efficiency, there is a great demand for the addition amount in order to achieve the standard flame retardant effect [12], but the performance of the matrix material will be reduced [13]. The above defects limit the use and promotion of MH. Fortunately, the surface modification of MH can significantly improve the dispersion and compatibility, and then improve the mechanical properties and flame retardancy of the composites [14].

Gallic acid (3,4,5-trihydroxybenzoic acid, GA) is one of the most important compounds of the hydrolysable polyphenols group, widely distributed in a variety of plant tissues [15,16], is commonly found in various plant-based foods and beverages [17]. Because of its antioxidant and antimicrobial properties, GA found applications in food, cosmetics, and pharmaceutical fields [18]. The three phenolic-OH groups and one carboxyl group make GA a good candidate to form stable complexes with metal ions [19]. Saha et al. investigated the behavior of a new two-component hydrogel of metal ions and GA synthesized at different proportions of the components [20]. Some studies even reported the possibility of GA and metal ions mutual detection based on the formation of stable complexes, for example the calorimetric detection of metal ions using GA silver nanoparticles [21] or the electrochemical detection of GA using a poly (melamine) film [22]. The availability and cost-effectiveness of GA make it suitable for FR applications. GA derivatives showed their efficiency as FR in epoxy resins [23] and polyurethane coatings [19].

To sum up, in this paper, magnesium hydroxide will be modified by the complex of gallic acid and  $\text{Fe}^{3+}$ . The interaction process of functional groups in biomass acid on MH surface was analyzed by Fourier infrared spectroscopy, scanning electron microscopy, X-ray powder diffraction and X-ray photoelectron spectroscopy. The proofed functionalized fillers will be further applied in EVA fire safety enhancement and the comprehensive properties of materials will be investigated.

## 2. Experimental

### 2.1. Materials

Ethylene vinyl acetate (EVA, UL00628) was purchased from Shandong zhongbo New Materials Co., Ltd. (Shandong, China); Magnesium hydroxide (MH) was obtained from Liaoning essence new material Limited by Share Ltd; Gallic acid (GA) and ferric chloride ( $\text{FeCl}_3$ ,  $\geq 99.0\%$ ) were provided by Tianjin Damao Chemical Reagent Factory.

### 2.2. Preparation of modified magnesium hydroxide

Firstly, 100 g of MH and 300 mL of deionized water located at a beaker (1 L) and stir at  $80^\circ\text{C}$  to disperse. Then, 1 g of GA is mixed with 100 mL of deionized water and added to the magnesium hydroxide solution, and then 1 g of  $\text{FeCl}_3$  is dissolved in 100 mL of deionized water. After the GA solution is added to the MH solution, continue stirring for 15 min, then add the  $\text{FeCl}_3$  solution and stir for 15 min, and then filter the obtained MH slurry and clean the filter cake. The above process was repeated twice to obtain gallic acid complex iron ion modified magnesium hydroxide (MH@Fe-GA),

put the obtained filter cake into the oven for drying for 12 h, grind it through the ball mill and collect it for standby (See Fig. 1).

### 2.3. Preparation of composite materials

Prepare the composite according to the formula in Table 1, set the front roll and rear roll of the open mill to  $100^\circ\text{C}$ , and obtain EVA/MH composite.

### 2.4. Characterization

The Fourier transform infrared (FTIR) spectra were performed on a Nicolet MNGNA-IR560 (Artisan Technology Group, Austin, TX, USA) with range of the spectral region from  $400\text{ cm}^{-1}$  and  $4000\text{ cm}^{-1}$  and used the attenuated total reflectance method (ATR). The scanning electron microscope (model: jeol JSM-6360 L V) produced by Hitachi, Japan was tested and the SEM image of magnesium hydroxide was obtained. X-ray diffractometer (XRD) tests was employed to XRD Analyzer with the magnesium hydroxide of D8 ADVANCE Bruker Germany, hydroxide, and the light source is Cu K  $\alpha$ . The scanning speed is  $5^\circ/\text{min}$ , and the  $2\theta$  angular scanning range is  $5^\circ\text{--}80^\circ$ . Manufactured using Kratos, UK, equipped with Al K $\alpha$  XPS spectra were obtained by X-ray photoelectron spectrometer of light source. Charge correction is carried out with  $\text{C}1s = 284.80\text{ eV}$  binding energy as the energy standard. Limiting oxygen index (LOI) measurements were carried out using Taiwan Songshu Testing Instrument Co., Ltd (model: ss-1005) in accordance with GB/T 2406–2009. The samples used for the test were of dimensions of  $126 \times 6.5 \times 3\text{ mm}^3$ . Vertical burning tests (UL94) were carried out using a Taiwan Songshu Testing Instrument Co., Ltd (model: ss-3001) in accordance with ASTM D3801–2010. The samples used for the test were of dimensions of  $130 \times 13 \times 3\text{ mm}^3$ . The cone calorimeter tests were carried out using a cone calorimeter (FTT, England, United Kingdom), following the ISO 5660–1:2015 standard procedures. The specimens were tested at a radiant heat flux of  $50\text{ kW/m}^2$ . The size of the sample is  $100 \times 100 \times 4\text{ mm}^3$ . The tensile property test measurements were carried out using Instron Engineering Corporation of the United States (model: 9250HV) in accordance with GB/T 528–2009. The test shall be carried out at the tensile speed of  $50\text{ mm/min}$  at room temperature. Each group of samples shall be tested for 5 times, and the average value and error value shall be taken. The impact performance test measurements were carried out using High Speed Rail Technology Co. Ltd (model: GJ-7045-MDL) in accordance with ISO 2932003. Each group of samples shall be tested for 5 times, and the average value and error value shall be taken. The STA449C thermal analyzer of NETZSCH Germany is used to measure MDH and MDH@Fe-PDA Thermal stability (Test conditions:  $\text{N}_2$  atmosphere, heating rate  $10^\circ\text{C/min}$ , temperature range  $40\text{--}800^\circ\text{C}$ ).

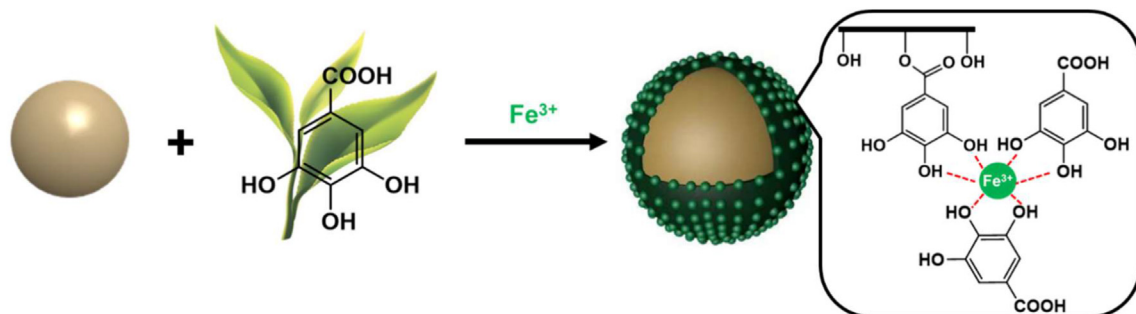


Fig. 1. Schematic diagram of gallic acid modified magnesium hydroxide (the brown sphere).

**Table 1**  
Formula of flame retardant EVA composites.

Samples	EVA/phr	MH/phr	GA/phr	FeCl <sub>3</sub> /phr
EVA/MH@Fe-GA(01)	100	150	3	0
EVA/MH@Fe-GA(02)	100	150	3	1.5
EVA/MH@Fe-GA(03)	100	150	3	3
EVA/MH@Fe-GA(04)	100	150	3	4.5
EVA/MH@Fe-GA(05)	100	150	3	6

### 3. Results and discussion

#### 3.1. Structural characterization of modified MH

The infrared absorption spectrum of MH before and after gallic acid modification is shown in Fig. 2. The absorption peak at 3694 cm<sup>-1</sup> comes from the stretching vibration absorption peak of -OH free on the surface of MH [24,25]. The peak at 3443 cm<sup>-1</sup> belongs to associated -OH stretching vibration. In plane deformation vibration absorption peak attributed to -OH at 1430 cm<sup>-1</sup> [20]. In the FTIR spectra of MH@Fe-GA, the peaks at 1820 cm<sup>-1</sup> and 1634 cm<sup>-1</sup> can be attributed to the stretching vibration absorption peak of C=O in gallic acid. MH@Fe-GA retained the peaks corresponding to MH and GA, and showed two additional peaks at 882 and 1487 cm<sup>-1</sup> [26] corresponding to the stretching vibration absorption peaks outside the C-H plane of the substituted aromatic ring. And two absorption peaks at 1320-1022 cm<sup>-1</sup> come from the bending vibration of C-H and O-H of phenolic hydroxyl in benzene ring [17]. The results showed that gallic acid was successfully grafted on the surface of magnesium hydroxide.

Furthermore, by comparing the SEM images, it can be observed that in the unmodified magnesium hydroxide powder of Fig. 3a, the agglomeration effect between the powders is obvious, and the particle size of the larger aggregate can reach tens of microns. However, in Fig. 3b, the particle size of the magnesium hydroxide powder modified by gallic acid is reduced, which has greatly reduced the agglomeration phenomenon between the magnesium hydroxide powders, which shows that, compared with unmodified magnesium hydroxide powder, the refinement degree of magnesium hydroxide powder modified by gallic acid is more significant. At the same time, the reduction of particle size of magnesium

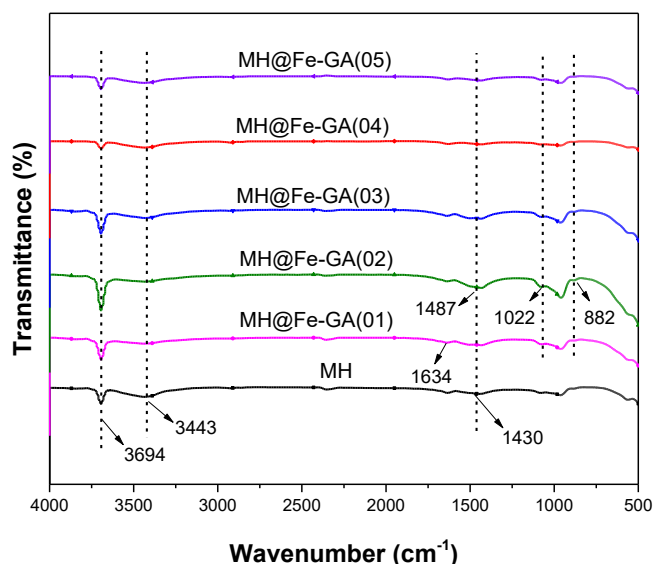


**Fig. 2.** Infrared spectra of magnesium hydroxide powder.

hydroxide powder will contribute to its dispersion in polymer matrices.

Fig. 4 is the XRD diagram of unmodified MH and magnesium hydroxide treated with gallic acid and iron. As it can be seen, the position of the characteristic peak of modified MH is consistent with that of unmodified MH, and no new characteristic peak appears, indicating that the modification process of gallic acid does not damage the crystal structure of MH. The diffraction angles are 12.14°, 38.02°, 50.89° and 58.71°, and there are strong characteristic peaks corresponding to (001), (101), (102) and (110) crystal planes of MH respectively. However, the intensity of the characteristic peak changes, and the ratio of I<sub>001</sub>/I<sub>101</sub> increases significantly. In MH crystal, the (001) crystal plane has weak polarity, while the (101) crystal plane has strong polarity. The ratio of diffraction peak intensity between MH (001) crystal plane and (101) crystal plane can reflect its surface polarity. After modification, I<sub>001</sub>/I<sub>101</sub> increases, indicating that the polarity of MH surface is weakened after modification, indicating that gallic acid is coated on the surface of MH particles [24,27].

Fig. 5 shows MH and MH@Fe-GA XPS full spectrum. As it can be seen, Mg, C and O elements appear in the six XPS spectra. And element C in MH may come from CO<sub>2</sub> in the surface adsorption environment. The electronic binding energy of these elements is shown in Fig. 5. Signals at 280.4 eV, 304.4 eV, 529.4 eV and 720.5 eV, 304.4 eV are C1s, Mg auger, O1s and Fe2p signals, respectively. It can be found that Fe2p signal only appears in MH@Fe-GA (02)-MH@Fe-GA (05) shows that Fe<sup>3+</sup> and GA ions are successfully complexed on MH.

#### 3.2. Flame retardancy of modified MH

In order to study the thermal stability and charring rate of EVA composites, we used thermogravimetric analysis to obtain the TGA curve at a heating rate of 10 °C/min in N<sub>2</sub> atmosphere. Fig. 6 shows the TGA curve of EVA and EVA composites. The TGA parameters are summarized in Table 2. EVA composites undergo two decompositions, the first decomposition occurs between 250 and 400 °C, and the weight loss in this stage is mainly due to the conversion and decomposition of acetic acid contained in EVA. The second decomposition occurs between 425 and 550 °C, and only the polyethylene chain in EVA is decomposed in this stage. In the second decomposition stage, GA and Fe<sup>3+</sup> modified MH were used, and its thermal decomposition temperature moved to higher temperature. In addition, the carbon residue rate of the composite material has changed significantly, and the carbon residue rate of the composite material has increased to a certain extent after adding Fe<sup>3+</sup>, which is due to the strong catalytic carbonization of Fe<sup>3+</sup> coordination GA compound to improve the carbon residue rate of EVA composite material.

The LOI value and UL-94 test grade result of the EVA composites are shown in Fig. 7. It can be seen that the LOI value of the EVA/MH composite material is 38.1%, which is a non-flammable material and has passed the V-0 level in the UL-94 test rating. Compared with EVA/MH, the LOI of EVA/MH@GA (01) has increased to 38.5%, which may be related to the better dispersibility of gallic acid modified MH. After the introduction of iron ions, the oxygen index of the EVA/MH composite material is reduced, and the more ions are introduced, the lower the oxygen index can be detected. This may be because the transition metal ions have a strong catalytic effect on the EVA matrix to ignite. At the same time, the UL-94 tests showed that all passed the V-0 in UL94 test rating. This should be attributed to the dehydration of MH releases amount of steam, dilute the concentration of oxygen and takes away heat [26,28].

The cone calorimetry test (CCT) has been used to evaluate the flammability of EVA composites. The results of the combustion test

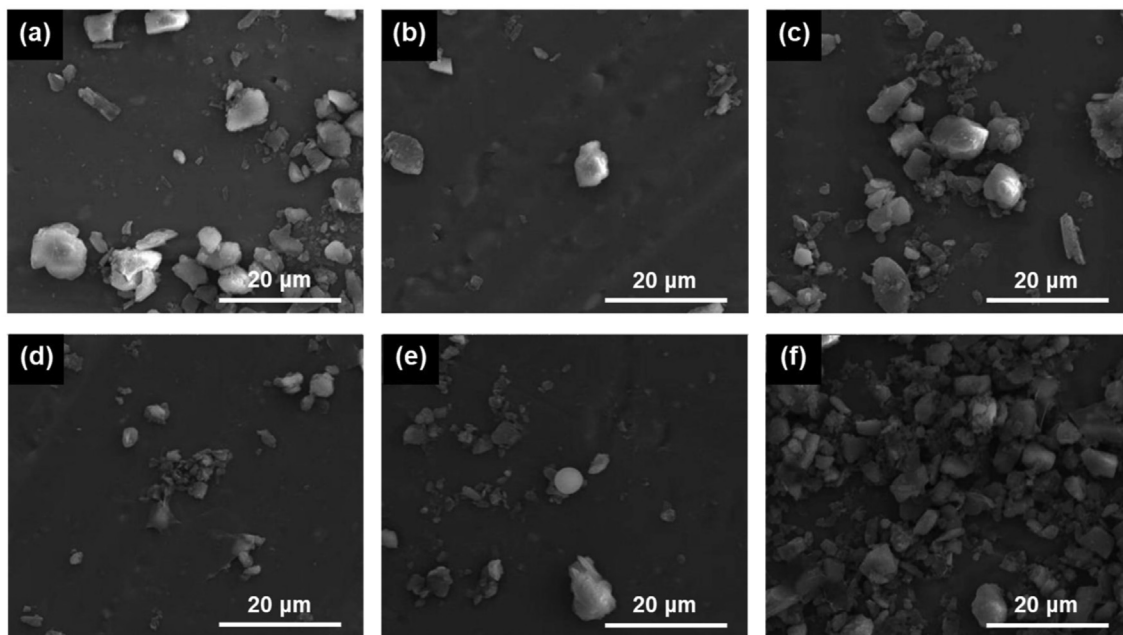


Fig. 3. SEM photo of magnesium hydroxide powder: (a) MH, (b) MH@Fe-GA (01), (c) MH@Fe-GA (02); (d) MH@Fe-GA (03), (e) MH@Fe-GA (04), and (f) MH@Fe-GA (05)

are shown in Fig. 8, including the heat release rate (HRR), total heat release (THR), smoke produce rate (SPR), total smoke production (TSP). Fig. 8 showed the HRR and TSP curves of both pure MH and modified MH composites. It can be seen that the pHRR of pure EVA is 1196 kW/m<sup>2</sup>. And the pure of EVA in fast combustion mode after ignition, a large amount of heat is released in a short time, and the heat release intensity reaches the highest. A sharp HRR peak of 1233 kW/m<sup>2</sup> appears at 155 s. The addition of MH in EVA composites results the pHRR decreased to 225 kW/m<sup>2</sup>. This is because MH itself has decalescence and decomposition ability. The heat release strength of EVA/MH composites decreases greatly, and the heat release rate becomes low. The EVA compound material modified by Fe<sup>3+</sup> and GA decrease of heat release intensity to a higher degree obviously, and the heat release rate becomes lower.

Furthermore, addition of MH@GA in EVA composites results the lower pHRR, which is reduced by 49.77% compared with that of EVA/MH composites. At the same time, the heat release rate in the middle and late stage of the whole combustion is very stable and the plateau period is very long. It is might be due to the remarkable catalytic carbonization property of Fe<sup>3+</sup>, which can form a better compact and succession protective carbon layer, and can effectively protect the EVA matrix from the influence of heat and combustible gases. Furthermore, with the appearance of carbon layer and MgO shell, the heat release rate decreases and the first peak decreases. However, the breakable carbon layer cannot block heat and oxygen highly efficiently, once again increasing the heat release rate. That is why some samples perform two heat release peaks. It is further found that the first peak of EVA/MH@Fe-GA (02) to EVA/MH@Fe-GA

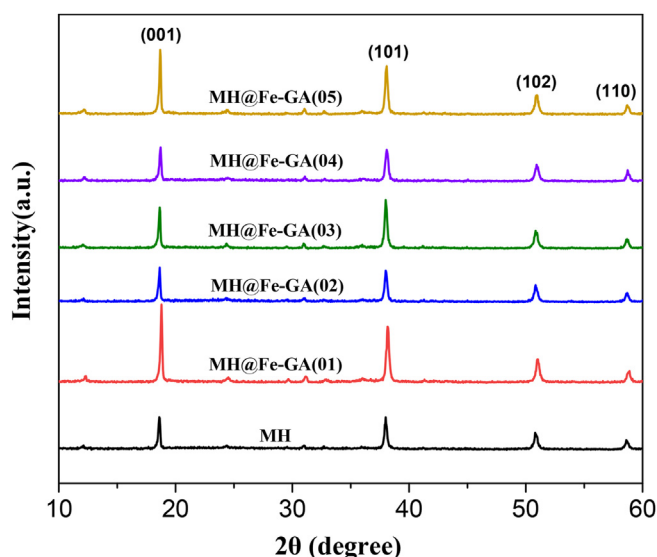


Fig. 4. XRD spectrum of magnesium hydroxide powder.

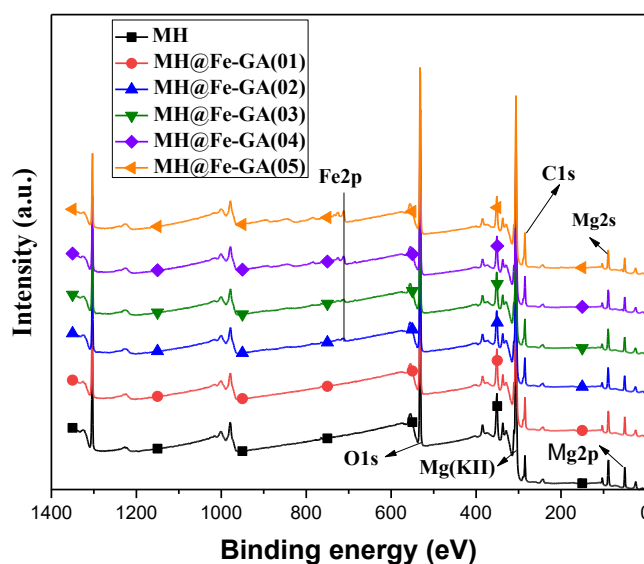


Fig. 5. XPS spectrum of magnesium hydroxide powder.

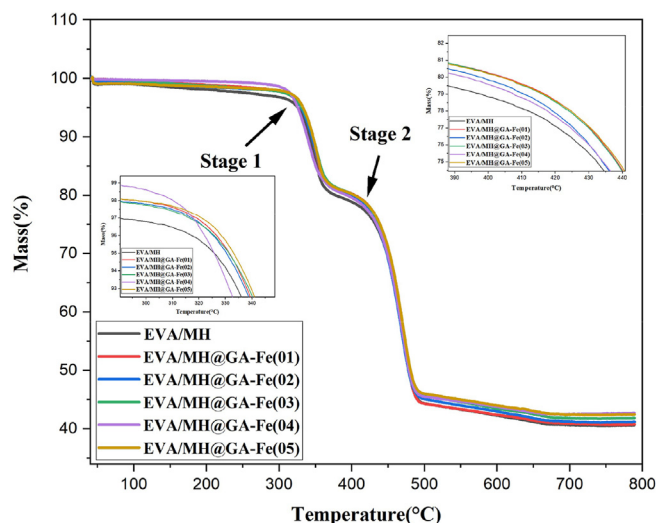


Fig. 6. TGA curves of EVA composites under  $N_2$  at heating rate of  $10\text{ }^\circ\text{C}/\text{min}$ .

**Table 2**  
TGA data of EVA composite.

Sample	$T_5$ wt% ( $^\circ\text{C}$ )	$T_{\text{max}}$ ( $^\circ\text{C}$ )	$C_{780}$ (%)
EVA	325	469	40.5
EVA/MH@GA-Fe(01)	331	470	40.7
EVA/MH@GA-Fe(02)	330	469	41.1
EVA/MH@GA-Fe(03)	331	468	41.8
EVA/MH@GA-Fe(04)	325	471	42.6
EVA/MH@GA-Fe(05)	333	469	42.4

(05) appeared earlier than the other two groups of composites, which is mainly due to the addition of  $\text{Fe}^{3+}$  making it easier for the material to form a protective carbon layer with high strength and good compactness due to the catalytic carbonization of  $\text{Fe}^{3+}$  in the combustion process, further indicating that the effective role of the residual carbon protective layer in the combustion process. In addition, the second peak of EVA/MH and EVA/MH@Fe-GA (01) composite is more obvious and higher than that of EVA/MH@Fe-GA (02) to EVA/MH@Fe-GA (05), which is because the MgO protective

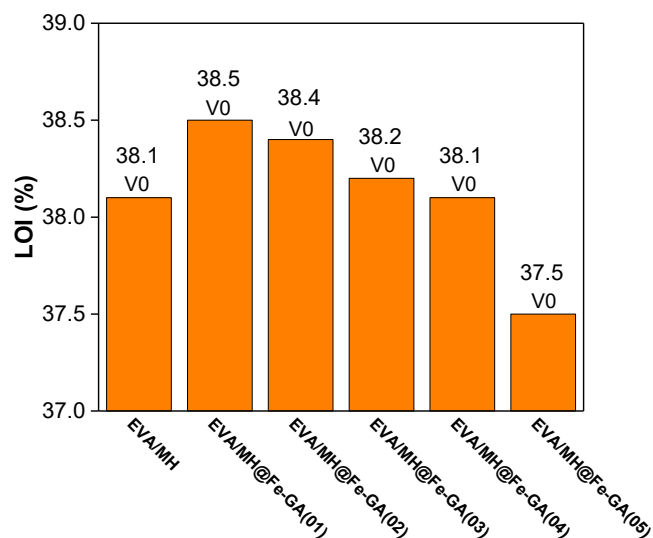


Fig. 7. LOI values and UL-94 test grade results of flame retardant EVA composites.

layer formed by magnesium hydroxide during combustion is relatively thin and brittle [27].

According to statistics, the human and animal deaths are mainly caused by deleterious and corrosive smoke produced by polymer materials during combustion. Therefore, it is very necessary to improve the smoke suppression performance of flame retardants. These smokes are mainly composed of aromatic intermediates and derivatives, which can be catalyzed by transition metals into stable carbon materials. Fig. 8 (a) and (b) compare EVA, EVA/MH and EVA/MH@Fe-GA smoke release rate (SPR) and total smoke release (TSP) of the seven groups of composites. It can be seen that when MH and MH@Fe-GA are incorporated, both TSP and SPR of the composites decreased significantly, especially the composite MH@Fe-GA (05). Compared with pure EVA, the SPR value decreased by 86% and TSP value decreased by 63%. The reason for the sharp decrease of SPR and TSP values is the catalytic carbonization of  $\text{Fe}^{3+}$ , which makes the composite easy to form a protective carbon layer with high strength and good compactness, which makes the carbon layer more stable, effectively inhibits the release of smoke and prevents the diffusion of combustible small molecular gases into the air. As it further can be seen, EVA/MH@Fe-GA is significantly lower than the other two curves. This is mainly due to the MgO shell formed after the thermal decomposition of magnesium hydroxide inhibits the release of smoke, but the shell is fragile and has limited inhibitory effect on the release of smoke, which cannot highly inhibit the release of smoke.

In fire accident, the threat of smoke has a more serious impact on human life safety. Generally, when a fire occurs in a general civil residence, the best escape time is within 3 min after the fire. Therefore, the less smoke is generated within 3 min, which is more favorable for humans to escape from the fire site. At 180 s, the total smoke emission of EVA, EVA/MH and EVA/MH@Fe-GA (05) composites was  $5.7\text{ m}^2$ ,  $1.8\text{ m}^2$  and  $1.4\text{ m}^2$  respectively. The total smoke emission of at 180 s is reduced by 75% compared with pure EVA, which is very beneficial to the escapees in case of fire.

In order to better study the carbon layer of composites, the digital images of CCT on the outer surface of residual carbon were analyzed. As can be seen from the photo of carbon residue in Fig. 9, obvious dendritic lines can be observed in the carbon residue after combustion. The outer surface of the residual carbon of EVA/MH composites presents a broken structure, which is due to the produced residual carbon layer is brittle and easy to crack. The residual carbon from  $\text{Fe}^{3+}$  and GA is comparatively integrated, which is mainly due to the catalytic carbonization of  $\text{Fe}^{3+}$ , producing more complete and dense carbon layers, as to produce more residual carbon. The existence of residual carbon will slow down the degradation rate of polymer by inhibiting most of oxygen and heat into the matrix and releasing it back to the gas phase, so as to reduce the fuel that can provide flame combustion in the combustion process [29].

Based on the above results and analysis, the flame-retardant mechanism of MH@Fe-GA in EVA composites are proposed in Fig. 10. In the gas phase, the combustion of polymer materials depends largely on the concentration of highly reactive free radicals (such as  $\text{H}\cdot$  and  $\text{OH}\cdot$ ), which can provide additional fuel to maintain the flame. MH@Fe-GA may slow down the free radical chain reaction by removing nearby  $\text{H}\cdot$  and  $\text{OH}\cdot$  free radicals, and the release of noncombustible gas caused by MH@Fe-GA degradation dilutes the concentration of flammable volatiles and oxygen, so as to promote flame extinguishing [9,30]. In the solidified phase,  $\text{Fe}^{3+}$  significantly catalyzes the formation of carbon residues. The dense carbon layer produced by catalytic carbonization can be used as a better thermal insulation barrier, so as to significantly reduce the heat transfer between “fuel” and oxygen in the flame area and combustion materials. The strong protective effect of the carbon

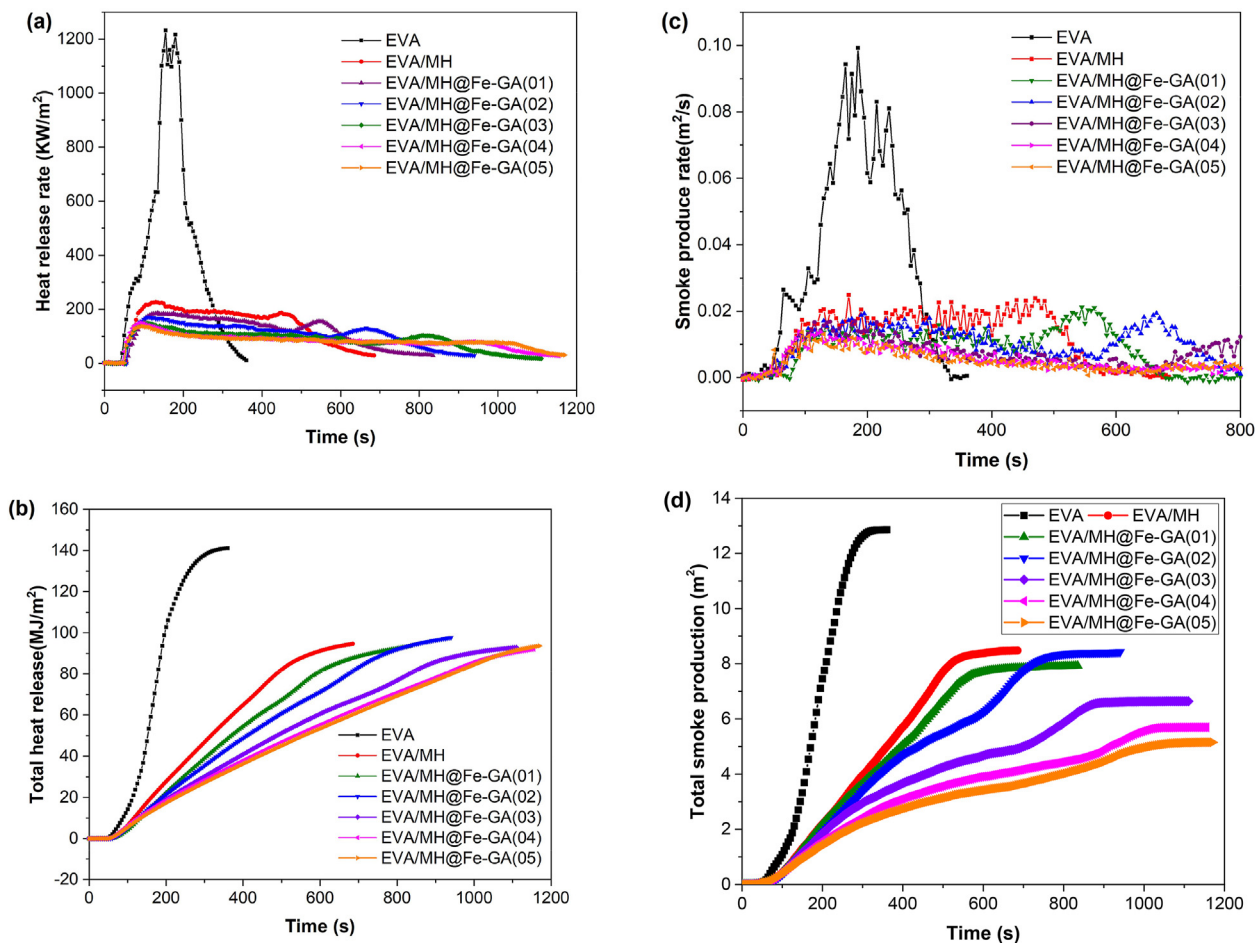


Fig. 8. CCT test results of EVA and flame retardant EVA Composites: (a) HRR, (b) THR, (c) SPR, and (d) THR.

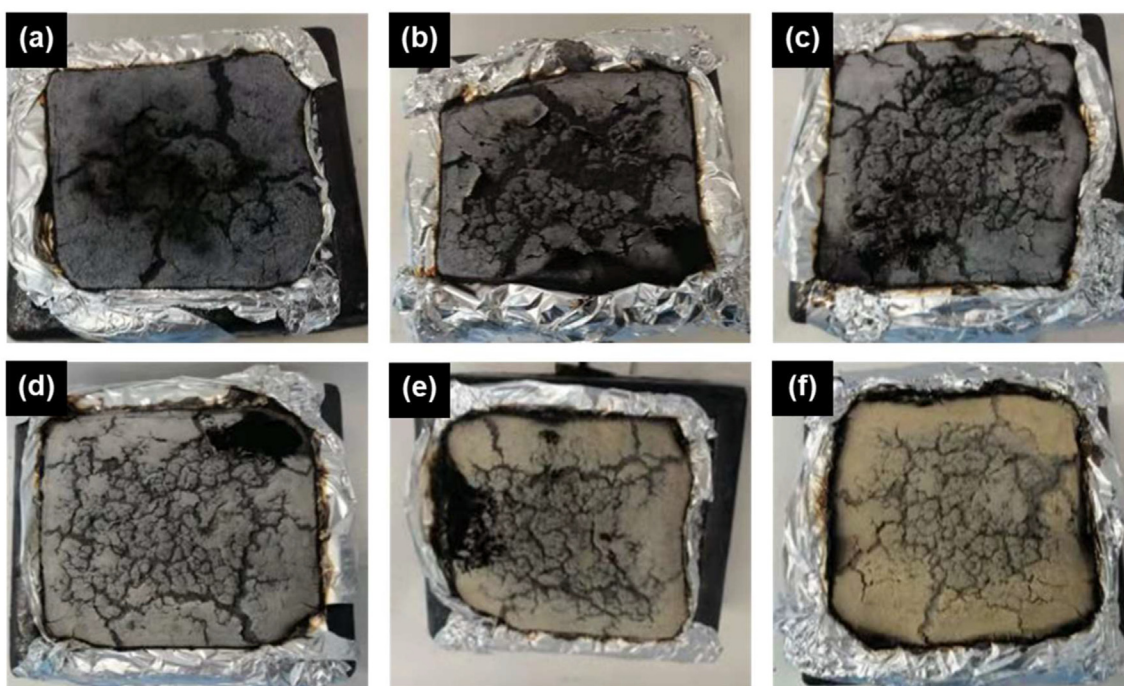


Fig. 9. Digital photo of cone calorimetric carbon residue: (a) EVA/MH, (b) EVA/MH@Fe-GA (01), (c) EVA/MH@Fe-GA (02), (d) EVA/MH@Fe-GA (03), (e) EVA/MH@Fe-GA (04) and (f) EVA/MH@Fe-GA (05).

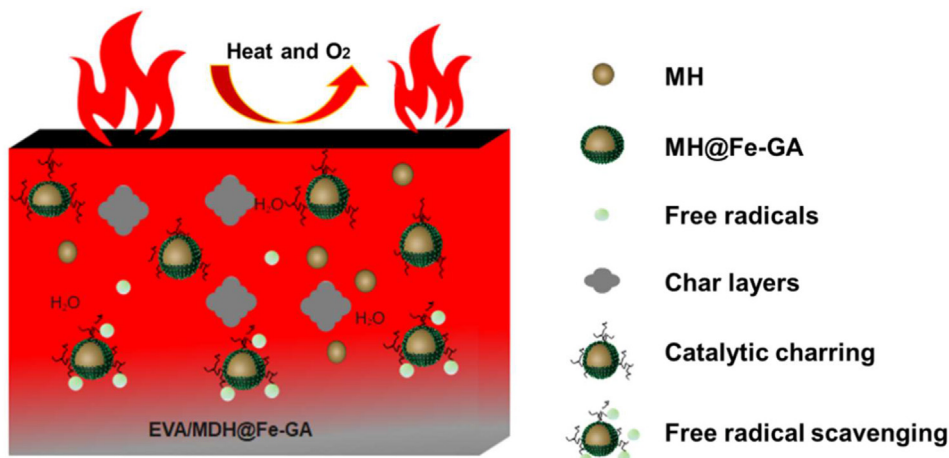


Fig. 10. Flame retardant mechanism of modified magnesium hydroxide.

layer may be one of the reasons for the improvement of flame retardancy.

### 3.3. Mechanical properties of EVA composites

Fig. 11 (a) shows the impact strength test results of flame retardant EVA composites. The tensile strength of flame retardant EVA composites added with modified magnesium hydroxide has been effectively improved. The highest impact strength of EVA/MH@Fe-GA is 37.8 MPa, which is 33% higher than that of EVA/MH composite, and other components are more than 28% higher than that of EVA/MH composite. Fig. 11 (b) shows the results of elongation at break of flame retardant EVA composite, and the elongation at break of flame retardant EVA composite has been significantly improved. The elongation at break of EVA/MH@Fe-GA (04) reached 81.9%, which was 144.5% higher than that of EVA/MH, indicating that the tensile properties of gallic acid modified EVA composites were significantly improved. The main reason for this improvement is that after gallic acid modification, the surface polarity, agglomeration degree and particle size of the powder are reduced, and the compatibility between the powder and the matrix material is improved, so as to improve the dispersion of magnesium hydroxide in the matrix. It is very helpful to improve the mechanical properties of EVA/MH flame retardant composites [31].

In order to study the dispersion of non modification MH particles and modification MH particles in the thermoplastic EVA matrix, the brittle fracture surface of EVA composites treated with liquid nitrogen was analyzed by SEM. Fig. 12 (a) and (b) is the sectional scanning picture of EVA composite material with unmodified MH. It can be seen from the picture that the non-functionalized MH is poorly dispersed in the thermoplastic EVA matrix, and blocks and particles of different sizes are clustered together. The boundary line between MDH particles and thermoplastic EVA matrix is clear, and it is not well immersed in the matrix. This may be because the non-modification MH particles have high external surface energy and strong external surface polarity, resulting in poor compatibility with the thermoplastic EVA matrix. The dispersion of GA modified MH powder is obviously improved, and the boundary line and surface contour between GA modified MH and thermoplastic material EVA matrix are relatively vague compared with EVA/MH matrix material. It is well immersed in EVA matrix, and the phenomenon of obvious agglomeration into large blocks is obviously improved. This may be due to GA coating on the surface of MH, reducing the external surface energy of MH,

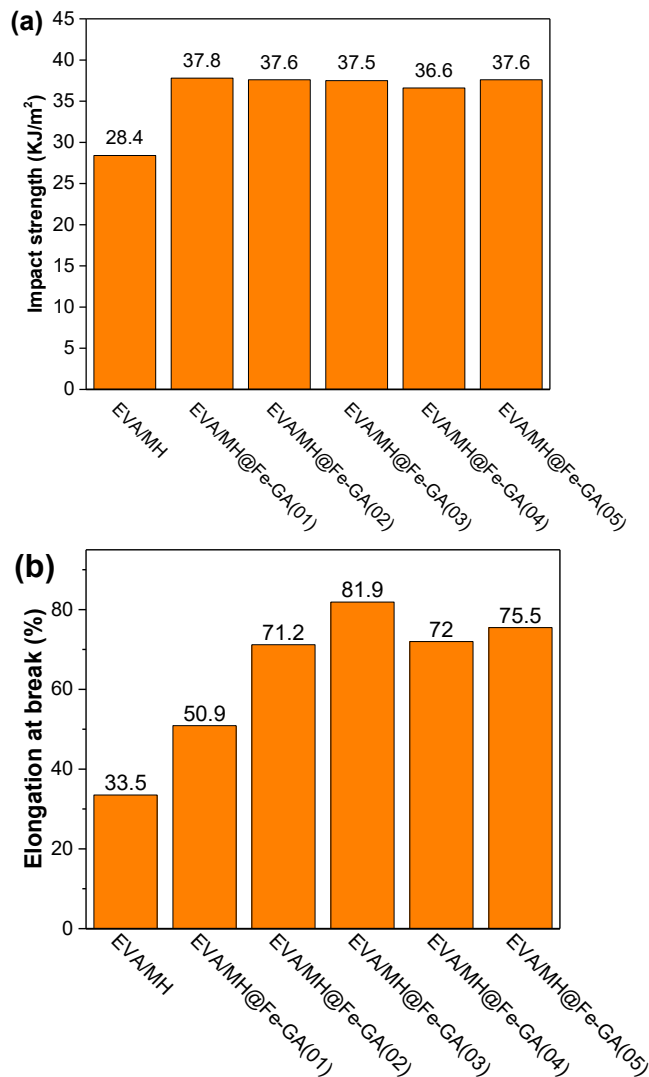


Fig. 11. Mechanical tests of flame-retardant EVA composites: (a) Impact strength; (b) Elongation at break.

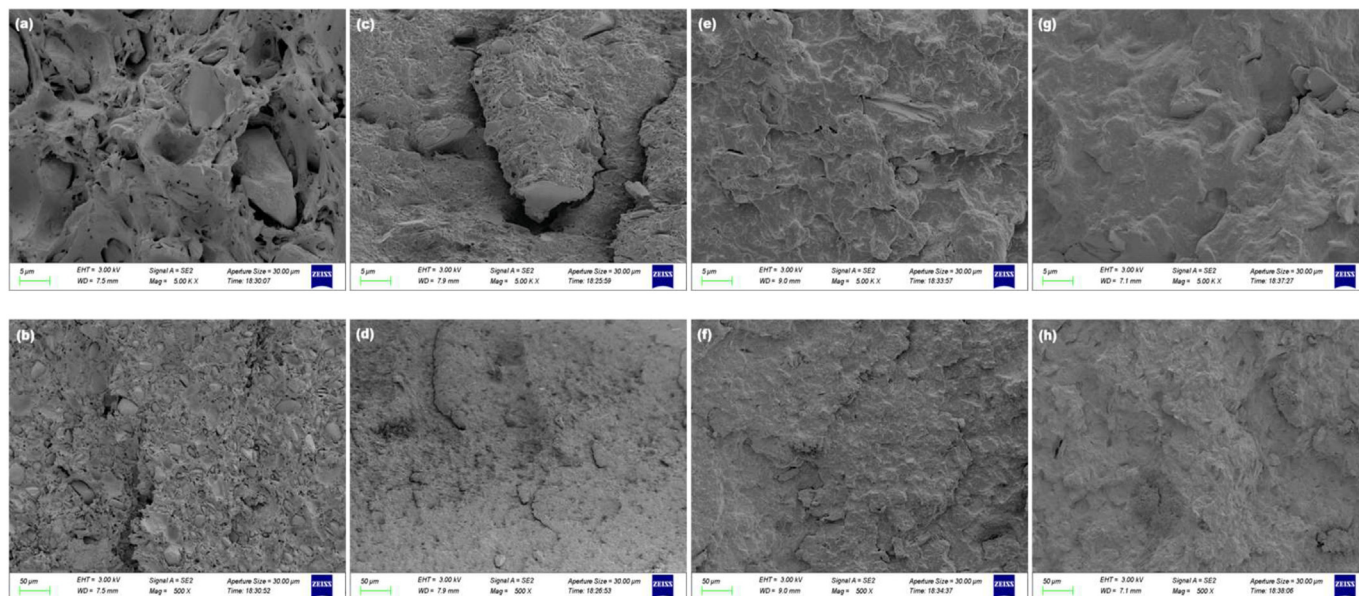


Fig. 12. SEM images: (a) and (b) EVA/MH; (c) and (d) EVA/MH@GA-Fe (01); (e) and (f) EVA/MH@GA-Fe (02); (g) and (h) EVA/MH@GA-Fe (03)

changing the surface polarity, and improving the compatibility with EVA matrix.

#### 4. Conclusions

In this article, the magnesium hydroxide modified by gallic acid complex iron (MH@Fe-GA) were used as flame retardant in EVA. The flame retardancy of EVA composites were significantly improved. It is concluded that magnesium hydroxide modified by gallic acid shows excellent flame retardant and smoke suppression properties. Typically, compared with neat EVA, the vertical combustion test of EVA composites modified by gallic acid successfully passed the V-0 grade, and the highest LOI value can reach 38.5%, and the pHRR of EVA/MH@Fe-GA decreased by 90.83%, TSP decreased by 86%, and the carbon residue was relatively complete. By observing the carbon layer structure after combustion, it is found that the improvement of flame retardant performance depends on the dense carbon layer promoted by iron ions, which effectively plays the role of heat insulation and oxygen isolation. Moreover, the mechanical properties of gallic acid modified EVA were significantly improved. Compared with EVA/MH, the impact strength of EVA/MH@Fe-GA increased by more than 28%, and the elongation at break increased by 144.5%. The improvement of mechanical properties is due to the reduction of surface polarity, agglomeration degree and particle size of the powder after gallic acid modification, and the better compatibility between the powder and the matrix material, so as to improve the dispersion of magnesium hydroxide in the matrix. It is found that the improvement of flame-retardant performance depends on the dense carbon layer promoted by iron ions, which effectively plays the role of heat insulation and oxygen isolation.

#### Declaration of competing interest

The authors declare that they have no known competing financial interests or personal relationships that could have appeared to influence the work reported in this paper.

#### Acknowledgement

This study was supported by the National Natural Science Foundation of China (grant number 51973124), Liao Ning Revitalization Talents Program (grant number XLYC2005002), “Jie Bang Gua Shuai” of science and technology Projects of Liaoning Province in 2021 (grant number 2021JH1/10400091) and Shenyang Science and Technology Program-Major Key Core Technology Project (grant number 20-202-1-15).

#### References

- [1] L. Liu, J. Hu, J. Zhuo, C. Jiao, S. Chen Xli, Synergistic flame retardant effects between hollow glass microspheres and magnesium hydroxide in ethylene-vinyl acetate composites, *Polym. Degrad. Stabil.* 104 (2014) 87–94.
- [2] E.N. Kalali, S. De Juan, X. Wang, S. Nie, R. Wang, D.-Y. Wang, Comparative study on synergistic effect of LDH and zirconium phosphate with aluminum trihydroxide on flame retardancy of EVA composites, *J. Therm. Anal. Calorim.* 121 (2) (2015) 619–626.
- [3] J. Liu, K. Zhou, G. Tang, B. Wang, Z. Gui, R.K.K. Yuen, et al., Synthesis of Co<sub>3</sub>(HPO<sub>4</sub>)<sub>2</sub>(OH)<sub>2</sub> nanosheets and its synergistic effect with intumescent flame retardants in ethylene-vinyl acetate copolymer, *Polym. Compos.* 39 (1) (2018) 238–246.
- [4] A. Battig, G. Sanchez-Olivares, D. Rockel, B. Maldonado-Santoyo Mschartel, Waste not, want not: the use of leather waste in flame retarded EVA, *Mater. Des.* (2021) 210.
- [5] J. Wang, H. Shi, P. Zhu, J. Wei Yao, Ammonium polyphosphate with high specific surface area by assembling zeolite imidazole framework in EVA resin: significant mechanical properties, migration resistance, and flame retardancy, *Polymers* 12 (3) (2020).
- [6] M.A. Oualha, N. Omri, R. Oualha, M.A. Nouioui, M. Abderrabba, N. Amdouni, et al., Development of metal hydroxide nanoparticles from eggshell waste and seawater and their application as flame retardants for ethylene-vinyl acetate copolymer (EVA), *Int. J. Biol. Macromol.* 128 (2019) 994–1001.
- [7] L. Shen, C. Shao, R. Li, Y. Xu, H. Li Jlin, Preparation and characterization of ethylene-vinyl acetate copolymer (EVA)-magnesium hydroxide (MH)-hexaphenoxycyclotriphosphazene (HPCTP) composite flame-retardant materials, *Polym. Bull.* 76 (5) (2018) 2399–2410.
- [8] H. Huang, M. Tian, L. Liu, L. Liang Wzhang, Effect of particle size on flame retardancy of Mg(OH)<sub>2</sub>-filled ethylene vinyl acetate copolymer composites, *J. Appl. Polym. Sci.* 100 (6) (2006) 4461–4469.
- [9] D. Yao, G. Yin, Q. Bi, X. Yin, N. Wang, D.Y. Wang, Basalt fiber modified ethylene vinyl acetate/magnesium hydroxide composites with balanced flame retardancy and improved mechanical properties, *Polymers* 12 (9) (2020).
- [10] Y. Wang, Z. Li, Y. Li, J. Wang, X. Liu, T. Song, et al., Spray-drying-assisted layer-by-layer assembly of alginate, 3-aminopropyltriethoxysilane, and magnesium hydroxide flame retardant and its catalytic graphitization in ethylene-vinyl acetate resin, *ACS Appl. Mater. Interfaces* 10 (12) (2018) 10490–10500.

- [11] T. Zheng, W. Xia, Y. Guo Jliu, Modified magnesium hydroxide encapsulated by melamine cyanurate in flame-retardant polyamide-6, *J. Polym. Res.* 27 (9) (2020).
- [12] J. Liu, K. Zhou, G. Tang, B. Wang, Z. Gui, R.K.K. Yuen, et al., Synthesis of Co<sub>3</sub>(HPO<sub>4</sub>)<sub>2</sub>(OH)<sub>2</sub> nanosheets and its synergistic effect with intumescent flame retardants in ethylene-vinyl acetate copolymer, *Polym. Compos.* 39 (1) (2018) 238–246.
- [13] M. Yao, H. Wu, H. Liu, Z. Zhou, T. Wang, Y. Jiao, et al., In-situ growth of boron nitride for the effect of layer-by-layer assembly modified magnesium hydroxide on flame retardancy, smoke suppression, toxicity and char formation in EVA, *Polym. Degrad. Stabil.* 183 (2021).
- [14] W. Zhang, X. Li, Z. Shan, Y. Wang Sxiao, Surface modification of magnesium hydroxide by wet process and effect on the thermal stability of silicone rubber, *Appl. Surf. Sci.* 465 (2019) 740–746.
- [15] G.R. Genwali, M. Acharya Pprajbhandari, Isolation of gallic acid and estimation of total phenolic content in some medicinal plants and their antioxidant activity, *Nepal J. Sci. Technol.* 14 (1) (2013) 95–102.
- [16] X.-H. Wang, X.-M. Cai Cli, Optimal extraction of gallic acid from *Suaeda glauca* bge. Leaves and enhanced efficiency by ionic liquids, *Int. J. Chem. Eng.* 2016 (2016), 5217802.
- [17] J. Bai, Y. Zhang, C. Tang, Y. Hou, X. Ai, X. Chen, et al., Gallic acid: pharmacological activities and molecular mechanisms involved in inflammation-related diseases, *Biomed. Pharmacother.* 133 (2021), 110985.
- [18] M. Sani Usman, M.Z. Hussein, S. Fakurazi, F.F. Masarudin Mjahmad Saad, Gadolinium-doped gallic acid-zinc/aluminium-layered double hydroxide/gold theranostic nanoparticles for a bimodal magnetic resonance imaging and drug delivery system, *In Nanomaterials* 7 (2017).
- [19] M. Patel, S. Mestry, S. Khuntia Spmhaske, Gallic acid-derived phosphorus-based flame-retardant multifunctional crosslinking agent for PU coating, *J. Coating Technol. Res.* 17 (1) (2020) 293–303.
- [20] A. Saha, B. Roy, A.K. Garai Anandi, Two-component thermoreversible hydrogels of melamine and gallic acid, *Langmuir* 25 (15) (2009) 8457–8461.
- [21] M. Farrokhnia, S. Karimi Sskarian, Strong hydrogen bonding of gallic acid during synthesis of an efficient AgNPs colorimetric sensor for melamine detection via dis-synthesis strategy, *ACS Sustain. Chem. Eng.* 7 (7) (2019) 6672–6684.
- [22] S.-H. Su Y-Lcheng, Sensitive and selective determination of gallic acid in green tea samples based on an electrochemical platform of poly(melamine) film, *Anal. Chim. Acta* 901 (2015) 41–50.
- [23] B.A. Howell, E.A. Oberdorfer Klostrander, Phosphorus flame retardants for polymeric materials from gallic acid and other naturally occurring multi-hydroxybenzoic acids, *International Journal of Polymer Science* 2018 (2018), 7237236.
- [24] H. Yan, X-h Zhang, L-q Wei, X-g Liu, B-s Xu, Hydrophobic magnesium hydroxide nanoparticles via oleic acid and poly(methyl methacrylate)-grafting surface modification, *Powder Technol.* 193 (2) (2009) 125–129.
- [25] X. Chen, J. Yu, S. Guo, S. Lu, M. Luo Zhe, Surface modification of magnesium hydroxide and its application in flame retardant polypropylene composites, *J. Mater. Sci.* 44 (5) (2009) 1324–1332.
- [26] Y. Lu, S. Wu Cxu, Mechanical, thermal and flame retardant properties of magnesium hydroxide filled poly(vinyl chloride) composites: the effect of filler shape, *Compos. Appl. Sci. Manuf.* 113 (2018) 1–11.
- [27] X. Wang, H. Pang, W. Chen, G. Lin Yning, Nanoengineering core/shell structured brucite@polyphosphate@amine hybrid system for enhanced flame retardant properties, *Polym. Degrad. Stabil.* 98 (12) (2013) 2609–2616.
- [28] N. Wang, H. Teng, X. Zhang, J. Zhang, L. Li, J. Zhang, et al., Synthesis of a carrageenan-iron complex and its effect on flame retardancy and smoke suppression for waterborne epoxy, *Polymers* 11 (10) (2019).
- [29] X. Wang, E.N. Kalali, J.-T. Wan, D.-Y. Wang, Carbon-family materials for flame retardant polymeric materials, *Prog. Polym. Sci.* 69 (2017) 22–46.
- [30] Q. Bi, D. Yao, G.-Z. Yin, J. You, X.-Q. Liu, N. Wang, et al., Surface engineering of magnesium hydroxide via bioinspired iron-loaded polydopamine as green and efficient strategy to epoxy composites with improved flame retardancy and reduced smoke release, *React. Funct. Polym.* 155 (2020).
- [31] R. Mosurkal, R. Kirby, W.S. Muller, J. Soares, J. wkumar, Simple green synthesis of polyborosiloxanes as environmentally-safe, non-halogenated flame retardant polymers, *Green Chem.* 13 (3) (2011).